Coherent Optical Pulse Dynamics in Nano-composite Plasmonic Bragg Gratings

I.R. Gabitov, A.O. Korotkevich, A.I. Maimistov, and J.B. McMahon

Abstract The propagation of solitary waves in a Bragg grating formed by an array of thin nanostructured dielectric films is considered. A system of equations of Maxwell–Duffing type, describing forward- and backward-propagating waves in such a grating, is derived. Exact solitary wave solutions are found, analyzed, and compared with the results of direct numerical simulations.

1 Introduction

The last decade has been a period of rapid progress in the field of photonic crystals [1, 2, 3, 4, 5, 6, 7, 8, 9, 10]. In particular, the one-dimensional case of a *resonant Bragg grating* [1, 2, 3, 4, 5] or a *resonantly absorbing Bragg reflector* (RABR) [6, 7, 8] has been studied extensively. In the simplest case, a resonant Bragg grating consists of a linear homogeneous dielectric medium containing an array of thin films with resonant atoms or molecules. The thickness of each film

I.R. Gabitov

Department of Mathematics, University of Arizona, 617 North Santa Rita Avenue, Tucson, AZ 85721, USA, gabitov@math.arizona.edu

L.D. Landau Institute for Theoretical Physics, Russian Academy of Sciences, 2 Kosygin Street, Moscow, 119334, Russian,

A.O. Korotkevich

L.D. Landau Institute for Theoretical Physics, Russian Academy of Sciences, 2 Kosygin Street, Moscow, 119334, Russian, kao@itp.ac.ru

A.I. Maimistov

Department of Solid State Physics, Moscow Engineering Physics Institute Moscow, 115409, Russian, maimistov@pico.miphi.ru

J.B. McMahon

Program in Applied Mathematics, University of Arizona, 617 North Santa Rita Avenue, P.O. Box 210089, Tucson, AZ 85721-0089, USA, jmcmahon@math.arizona.edu

is much less than the wavelength of the electromagnetic wave propagating through such a structure. The interaction of ultra-short pulses and films embedded with two-level atoms has been studied by Mantsyzov et al. [1, 2, 3, 4, 5] in the framework of the two-wave reduced Maxwell–Bloch model and by Kozhekin et al. [6, 7, 8]. These works demonstrated the existence of a 2π-pulse of self-induced transparency in such structures [1, 4, 6]. It was also found [8] that bright solitons, as well as dark ones, can exist in the prohibited spectral gap, and that bright solitons can have arbitrary pulse area.

If the density of two-level atoms is very high, then the near-dipole–dipole interaction is noticeable and should be accounted for in the mathematical model. The effect of the dipole–dipole interaction on the existence of gap solitons in a resonant Bragg grating was studied in [10]; details can be found in [9]. Recent numerical simulations have yielded unusual solutions known as *zoomerons* [11]. The optical "zoomeron" was discovered and investigated recently [12] in the context of the resonant Bragg grating. These works also contain careful construction of the underlying mathematical model, which is derived from first principles. A "zoomeron" is a localized pulse which is similar to an optical soliton, except that its velocity oscillates around some mean value.

Recent advances in nano-fabrication have allowed for the creation of nano-composite materials, and these have the ability to sustain nonlinear plasmonic oscillations. These materials have metallic nano-particles embedded in them [13, 14, 15]. In this chapter, we consider a dielectric material, into which thin films containing metallic nano-particles have been inserted. These thin films are spaced periodically along the length of the dielectric, so that the Bragg-prohibited spectral gap is centered at the plasmonic resonance frequency of the nano-particles. We derive governing equations for the slowly varying envelopes of two counter-propagating electromagnetic waves and of the plasmonic oscillation-induced medium polarization. We find that this system of equations has the form of the two-wave Maxwell–Duffing model. We find exact solutions of this system and demonstrate that, in contrast to conventional 2π-pulses, they have nonlinear phase. We show that the stability of these solutions is sensitive to perturbation of this phase. We also study the collisions of these pulses and find that the outcomes of such collisions are highly dependent on relative phase.

There are three natural mechanisms of dissipation of energy in nanostructured Bragg gratings. The first mechanism is damping of the plasmonic oscillations, occurring within metallic nano-particles. In our work, we assume that the characteristic pulse duration is shorter than the characteristic time for these losses, and therefore, this type of loss can be neglected. The second source of dissipation is the result of irregularities in realistic gratings. Due to these irregularities, there is incomplete return of energy from the grating to the optical field during the field-grating interaction. As a result, non-returned energy that remains in the grating will be dissipated. The third mechanism is due to the presence of inhomogeneous broadening of the absorption line. In this case, the energy of the field is absorbed and redistributed among oscillators due to the phase modulation of the pulse. The range

of resonant frequencies of these excited oscillators is broader than the bandwidth of the optical field pulse. The energy of the oscillating particles which are outside that bandwidth will be dissipated. The material presented here is an essential starting point for work toward understanding the physics of these last two dissipation mechanisms for solitary pulses (dissipative solitons) in Bragg gratings with embedded nano-particles.

2 Basic Equations

We consider a grating formed by an array of thin films which are embedded in a linear dielectric medium. In our derivation of the governing equations, we follow [1, 2, 3, 4, 5, 6, 7, 8], wherein Bragg resonance arises if the distance between successive films is $a = (\lambda/2)m$, $m = 1, 2, 3, \ldots$. To obtain the governing equations, we apply the transfer-operator approach, as presented below.

2.1 Transfer-Operator Approach

Let us consider ultra-short optical pulse propagation along the X-direction of a periodic array of thin films, which are placed at points $\ldots, x_{n-1}, x_n, x_{n+1}, \ldots$ (Fig. 1). The medium between the films has dielectric permittivity ε. Hereafter, to be definite, we consider a TE-wave whose electric field component is parallel to the layers. All results can be easily generalized to the case of TM-polarized waves.

It is convenient to represent the electric and magnetic strengths E, H and the polarization of the two-level atoms ensemble P in the form of Fourier integrals
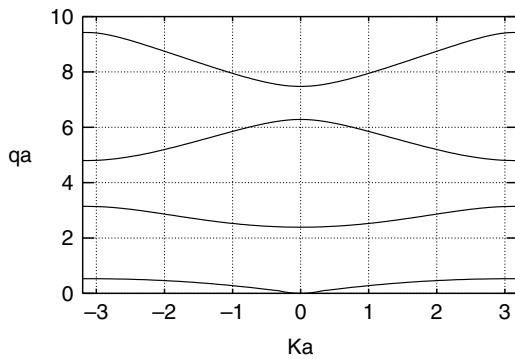

Fig. 1 An example of band structure, where inclusions are linear oscillators

$$\mathbf{E}(x,z,t) = (2\pi)^{-2} \int\limits_{-\infty}^{\infty} \exp[-\mathrm{i}\omega t + \mathrm{i}\beta z]\mathbf{E}(x,\beta,\omega)\mathrm{d}t\ \mathrm{d}z,$$

$$\mathbf{H}(x,z,t) = (2\pi)^{-2} \int\limits_{-\infty}^{\infty} \exp[-\mathrm{i}\omega t + \mathrm{i}\beta z]\mathbf{H}(x,\beta,\omega)\mathrm{d}t\ \mathrm{d}z,$$

$$\mathbf{P}(x_n,z,t) = (2\pi)^{-2} \int\limits_{-\infty}^{\infty} \exp[-\mathrm{i}\omega t + \mathrm{i}\beta z]\mathbf{P}(x_n,\beta,\omega)\mathrm{d}t\ \mathrm{d}z.$$

Outside the films, the Fourier components of the vectors $\mathbf{E}(x,\beta,\omega)$ and $\mathbf{H}(x,\beta,\omega)$ are defined by the Maxwell equations. At points x_n, these values are defined from continuity conditions. Thus, the TE-wave propagation can be described by the following system:

$$\frac{\mathrm{d}^2 E}{\mathrm{d}x^2} + \left(k^2\varepsilon - \beta^2\right) E = 0, \tag{1}$$

$$H_x = -(\beta/k)E, \quad H_z = -(\mathrm{i}/k)\mathrm{d}E/\mathrm{d}x, \quad E_y = E,$$

with boundary conditions [16, 17]

$$E(x_n - 0) = E(x_n + 0), \quad H_z(x_n + 0) - H_z(x_n - 0) = 4\mathrm{i}\pi k P_y(x_n,\beta,\omega), \tag{2}$$

where $k = \omega/c$. The solutions of (1) in the intervals $x_n < x < x_{n+1}$ can be written as

$$E(x,\beta,\omega) = A_n(\beta,\omega)\exp[\mathrm{i}q(x-x_n)] + B_n(\beta,\omega)\exp[-\mathrm{i}q(x-x_n)],$$

$$H_z(x,\beta,\omega) = qk^{-1}\left\{A_n(\beta,\omega)\exp[\mathrm{i}q(x-x_n)] - B_n(\beta,\omega)\exp[-\mathrm{i}q(x-x_n)]\right\},$$

where $q = \sqrt{k^2\varepsilon - \beta^2}$. Hence, the amplitudes A_n and B_n completely determine the electromagnetic field in a RABR. Let us consider the point x_n. The electric field at $x = x_n - \delta$ ($\delta << a$) is defined by amplitudes $A_n^{(L)}$ and $B_n^{(L)}$, and the field at $x = x_n + \delta$ is defined by $A_n^{(R)}$ and $B_n^{(R)}$. Continuity conditions (1) result in the following relations between these amplitudes:

$$A_n^{(R)} + B_n^{(R)} = A_n^{(L)} + B_n^{(L)},$$

$$A_n^{(R)} - B_n^{(R)} = A_n^{(L)} - B_n^{(L)} + 4\pi\mathrm{i}k^2 q^{-1} P_{\mathrm{S},n},$$

where $P_{\mathrm{S},n} = P_{\mathrm{S}}(A_n^{(R)} + B_n^{(R)})$ is the surface polarization of a thin film at point x_n. This is induced by the electrical field inside the film. Thus we find

$$A_n^{(R)} = A_n^{(L)} + 2\pi\mathrm{i}k^2 q^{-1} P_{\mathrm{S},n}, \quad B_n^{(R)} = B_n^{(L)} - 2\pi\mathrm{i}k^2 q^{-1} P_{\mathrm{S},n}. \tag{3}$$

Taking into account the strength of the electric field outside the films, we write

$$A_{n+1}^{(L)} = A_n^{(R)} \exp(\mathrm{i}qa), \quad B_{n+1}^{(L)} = B_n^{(R)} \exp(-\mathrm{i}qa). \tag{4}$$

If the vectors $\psi_n^{(L)} = (A_n^{(L)}, B_n^{(L)})$ and $\psi_n^{(R)} = (A_n^{(R)}, B_n^{(R)})$ are introduced, then the relations (3) can be represented as

$$\psi_n^{(R)} = \widehat{U}_n \psi_n^{(L)},$$

where $\widehat{U}_n$ is the *transfer-operator* of the vector $\psi_n^{(L)}$ through the film located at point x_n. In the general case, $\widehat{U}_n$ is a nonlinear operator. The relations (4) are represented in the vectorial form

$$\psi_{n+1}^{(L)} = \widehat{V}_n \psi_n^{(R)},$$

where the linear operator $\widehat{V}_n$ transfers the vector $\psi_n^{(R)}$ between adjacent thin films and is represented by the diagonal matrix

$$\widehat{V}_n = \begin{pmatrix} \exp(\mathrm{i}qa) & 0 \\ 0 & \exp(-\mathrm{i}qa) \end{pmatrix}.$$

In this manner, we define the nonlinear transfer-operator of the vector $\psi_n^{(L)}$ through an elementary cell of RABR:

$$\psi_{n+1}^{(L)} = \widehat{V}_n \widehat{U}_n \psi_n^{(L)} = \widehat{T}_n \psi_n^{(L)}. \tag{5}$$

The transfer-operator approach is frequently used in models of one-dimensional photonic crystals made of linear media, e.g., distributed feedback structures [18].

In (5), the upper index can be omitted, and the equation can be rewritten as the following recurrence relations:

$$A_{n+1} = A_n \exp(\mathrm{i}qa) + 2\pi \mathrm{i}k^2 q^{-1} P_{\mathrm{S},n} \exp(\mathrm{i}qa), \tag{6}$$
$$B_{n+1} = B_n \exp(-\mathrm{i}qa) - 2\pi \mathrm{i}k^2 q^{-1} P_{\mathrm{S},n} \exp(-\mathrm{i}qa). \tag{7}$$

These recurrence relations are exact, since no approximations (e.g., the approximation of the slowly varying envelope of electromagnetic pulses or the long-wave approximation) have been employed. Furthermore, the surface polarization of a thin film could be calculated via various suitable models. Here we follow the works of Mantsyzov et al. [1, 2, 3, 4, 5], Kozhekin et al. [6, 7], and Kurizki et al. [8, 9], where the two-level atom model has been used.

2.2 Linear Response Approximation

To demonstrate that the RABR is a true gap medium, it is appropriate to obtain the electromagnetic wave spectrum through a linear response approximation. In the general case, we can use the following expression for the polarization:

$$P_{S,n} = \chi(\omega)(A_n^{(R)} + B_n^{(R)}). \tag{8}$$

Substitution of this formula into (6) and (7) yields

$$A_{n+1} = (1 + i\rho)A_n \exp(iqa) + i\rho B_n \exp(iqa), \tag{9}$$

$$B_{n+1} = (1 - i\rho)B_n \exp(-iqa) - i\rho A_n \exp(-iqa). \tag{10}$$

Here $\rho = \rho(\omega) = 2\pi k^2 q^{-1}\chi(\omega) = 2\pi\omega c^{-1}\varepsilon^{-1/2}\chi(\omega)$. We employ an ansatz in which the wave is a collective motion of the electrical field in the grating. Hence

$$A_n = A\exp(ikna), \qquad B_n = B\exp(ikna). \tag{11}$$

Equations (9) and (10) show that the wave amplitudes, A and B, satisfy the following linear system of equations:

$$A\exp(iKa) = (1 + i\rho)A\exp(iqa) + i\rho B\exp(iqa), \tag{12}$$

$$B\exp(iKa) = (1 - i\rho)B\exp(-iqa) - i\rho A\exp(-iqa). \tag{13}$$

A non-trivial solution of this system exists if, and only if, the determinant is equal to zero, i.e.,

$$\det \begin{pmatrix} (1 + i\rho)\exp(iqa) - \exp(iKa) & i\rho\exp(iqa) \\ -i\rho\exp(-iqa) & (1 - i\rho)\exp(-iqa) - \exp(iKa) \end{pmatrix} = 0. \tag{14}$$

If we define

$$Z = \exp(iKa),$$

$$G = (1 + i\rho)\exp(iqa) = (\cos qa - \rho\sin qa) + i(\rho\cos qa + \sin qa),$$

then (14) can be rewritten as the following equation in Z:

$$Z^2 - (G + G^*)Z + 1 = 0.$$

This equation has solutions

$$Z_\pm = \mathrm{Re}\ G \pm i\sqrt{1 - (\mathrm{Re}\ G)^2}.$$

If $\mathrm{Re}G \leq 1$, then $\mathrm{Re}G \pm i\sqrt{1 - (\mathrm{Re}G)^2} = \cos Ka + i\sin Ka$. Hence the wave-numbers, $K_\pm$, are real-valued and satisfy the transcendental equation

$$\cos Ka = \cos qa - \rho\sin qa. \tag{15}$$

If $\mathrm{Re}G > 1$, then the roots of (14) are real. In this case, the wave-numbers, $K_\pm$, are purely imaginary. The condition $\mathrm{Re}G > 1$ defines the frequencies of the forbidden zone. The waves with these frequencies cannot propagate in the grating. The boundaries of this forbidden zone are defined by

$$\cos qa - \rho \sin qa = 1. \tag{16}$$

The model of the resonant system, containing the thin films, defines the explicit form of the function $\rho = \rho(\omega)$. The form of $\rho(\omega)$ determines the dispersion relation (15). It should be noted that this dispersion relation ensures a series of gaps in the electromagnetic wave spectrum. Figure 1 represents an example of such a band structure when the inclusions are linear oscillators.

2.3 Long-Wave and Weak Nonlinearity Approximations

We can transform the exact equations (6) and (7) into differential equations by using the long-wave approximation. To do so, we introduce the field variables

$$A(x) = \sum_n A_n \delta(x - x_n), \quad B(x) = \sum_n B_n \delta(x - x_n),$$

$$P(x) = \sum_n P_{S,n} \delta(x - x_n).$$

Using the integral representation of a Dirac delta-function,

$$\delta(x) = (2\pi)^{-1} \int_{-\infty}^{\infty} \exp(ikx) dk,$$

we obtain the following expression:

$$A(x) = (2\pi)^{-1} \sum_n A_n \int_{-\infty}^{\infty} \exp[ik(x - x_n)] dk$$

$$= (2\pi)^{-1} \int_{-\infty}^{\infty} \exp(ikx) \sum_n A_n \exp(-ikx_n) dk.$$

It follows that the Fourier transform of $A(x)$ is then

$$A(k) = \sum_n A_n \exp(-ikx_n) = \sum_n A_n \exp(-ikan),$$

and that the Fourier transforms of $B(x)$ and $P(x)$ are

$$B(k) = \sum_n B_n \exp(-ikan), \quad P(k) = \sum_n P_{S,n} \exp(-ikan),$$

respectively.

The form of these spatial Fourier components ensures periodicity in k. For example,

$$A(k) = \sum_n A_n \exp(-ikan)\exp(\pm 2\pi i n)$$

$$= \sum_n A_n \exp(-ikan \pm 2\pi i n) \tag{17}$$

$$= \sum_n A_n \exp[-ian(k \pm 2\pi/a)] = A(k \pm 2\pi/a).$$

From the recurrence equations (6) and (7), we have

$$A(k)\exp(ika) = A(k)\exp(iqa) + i\kappa P(k)\exp(iqa),$$
$$B(k)\exp(ika) = B(k)\exp(-iqa) - i\kappa P(k)\exp(-iqa),$$

or

$$[\exp\{ia(k-q)\} - 1]A(k) = i\kappa P(k), \tag{18}$$
$$[\exp\{ia(k+q)\} - 1]B(k) = -i\kappa P(k). \tag{19}$$

The linear approximation $P(k) = \chi(\omega)[A(k) + B(k)]$ for polarization again leads us to the linear dispersion law (14). The system of equations (18) and (19) is equivalent to the discrete equations (6) and (7). Up to this point, we have made no approximations other than the assumption on the width of the thin films.

If the thin film array was absent, then the dispersion relation would be

$$\cos ka = \cos qa.$$

In that case, the wave with amplitude $A(k)$ has $k = q$, indicating propagation to the right, while the wave with amplitude $B(k)$ has $k = -q$, indicating propagation in the opposite direction. Let us suppose that the polarization of the thin film array produces little change in wave vectors, i.e., for the right-propagating wave, the wave vector is $k = q + \delta k$, and for the opposite wave, the wave vector is $k = -q + \delta k$. If we set the value of q to be near one of the Bragg resonances, say $q = 2\pi/a + \delta q$, where $\delta q \ll 2\pi/a$, then (6) and (7) take the form

$$[\exp(ia\delta k) - 1]A(q + \delta k) = i\kappa P(q + \delta k),$$
$$[\exp(ia\delta k) - 1]B(-q + \delta k) = -i\kappa P(-q + \delta k).$$

By virtue of the periodicity conditions (17), these equations can be rewritten as

$$[\exp(ia\delta k) - 1]A(\delta q + \delta k) = i\kappa P(\delta q + \delta k),$$
$$[\exp(ia\delta k) - 1]B(-\delta q + \delta k) = -i\kappa P(-\delta q + \delta k).$$

After the change of variables $\delta k = \delta\tilde{k} \pm \delta q$, we have

$$\left[\exp\{ia(\delta\tilde{k} - \delta q)\} - 1\right]A(\delta\tilde{k}) = i\kappa P(\delta\tilde{k}), \tag{20}$$
$$\left[\exp\{ia(\delta\tilde{k} + \delta q)\} - 1\right]B(\delta\tilde{k}) = -i\kappa P(\delta\tilde{k}). \tag{21}$$

The long-wave approximation means that non-zero values of the spatial Fourier amplitudes are located near the zero value of the argument. Suppose that $a\delta\tilde{k}$ is small enough so that $\exp(ia(\delta\tilde{k}+\delta q)) \approx 1 + ia(\delta\tilde{k}+\delta q)$. Then, we replace (20) and (21) with the approximate equations

$$ia(\delta\tilde{k} - \delta q)A(\delta\tilde{k}) = i\kappa P(\delta\tilde{k}), \tag{22}$$

$$ia(\delta\tilde{k} + \delta q)B(\delta\tilde{k}) = -i\kappa P(\delta\tilde{k}). \tag{23}$$

Now, if we return to the spatial variable, (22) and (23) lead us to the equations of coupled-wave theory:

$$\frac{\partial A}{\partial x} = i\delta q A(x) + i\kappa a^{-1}P(x), \tag{24}$$

$$\frac{\partial B}{\partial x} = -i\delta q B(x) - i\kappa a^{-1}P(x). \tag{25}$$

In these equations, the fields $A(x), B(x), P(x)$ and the parameters δq, κ are functions of the frequency ω. To obtain the final system of equations in the spatial and time variables, we carry out an inverse Fourier transform. We now assume that the envelopes of the electromagnetic waves vary slowly in time [12]. This approximation simplifies the system of coupled wave equations under consideration.

2.4 Slowly Varying Envelope Approximation

In the slowly varying envelope approximation, we assume that the approximated fields are inverse Fourier transforms of narrow wave packets, i.e., they are quasi-harmonic waves [12]. For example, the quasi-harmonic wave form of the electric field is

$$E(x,t) = \mathscr{E}(x,t)\exp[-i\omega_0 t],$$

where ω_0 is the carrier wave frequency. The electric field, $E(x,t)$, and the Fourier components of the envelope, $\mathscr{E}(x,t)$, of the pulse are related by

$$E(x,t) = (2\pi)^{-1}\int_{-\infty}^{\infty} \widetilde{E}(x,\omega)\exp(-i\omega t)d\omega$$

$$= (2\pi)^{-1}\int_{-\infty}^{\infty} \widetilde{\mathscr{E}}(x,\omega)\exp[-i(\omega+\omega_0)t]d\omega$$

$$= (2\pi)^{-1}\int_{-\infty}^{\infty} \widetilde{\mathscr{E}}(x,\omega-\omega_0)\exp(-i\omega t)d\omega,$$

where the function $\widetilde{E}(x,\omega)$ is non-zero if $\omega \in (\omega_0 - \Delta\omega, \omega_0 + \Delta\omega)$, with $\Delta\omega \ll \omega_0$. Hence, $\widetilde{E}(x,\omega + \omega_0) = \widetilde{\mathscr{E}}(x,\omega)$. Thus, if we have some relation for $\widetilde{E}(x,\omega)$, then the analogous relation for $\widetilde{\mathscr{E}}(x,\omega)$ can be found by making the replacement $\omega \mapsto \omega_0 + \omega$ in all functions of ω.

Let

$$A(x,t) = \mathscr{A}(x,t)\exp(-i\omega_0 t), \quad B(x,t) = \mathscr{B}(x,t)\exp(-i\omega_0 t),$$
$$P(x,t) = \mathscr{P}(x,t)\exp(-i\omega_0 t).$$

From (24) and (25), it follows that the Fourier components $\mathscr{A}(x,\omega), \mathscr{B}(x,\omega)$, and $\mathscr{P}(x,\omega)$ satisfy

$$\frac{\partial \mathscr{A}}{\partial x}(x,\omega) = i\delta q(\omega_0 + \omega)\mathscr{A}(x,\omega) + i\kappa(\omega_0 + \omega)a^{-1}\mathscr{P}(x,\omega), \quad (26)$$

$$\frac{\partial \mathscr{B}}{\partial x}(x,\omega) = -i\delta q(\omega_0 + \omega)\mathscr{B}(x,\omega) - i\kappa(\omega_0 + \omega)a^{-1}\mathscr{P}(x,\omega). \quad (27)$$

Since $\mathscr{A}$, $\mathscr{B}$, and $\mathscr{P}$ are non-zero for $\omega \ll \omega_0$, one can use the expansions:

$$\delta q(\omega_0 + \omega) \approx q_0 - 2\pi/a + q_1\omega + q_2\omega^2/2, \quad \kappa(\omega_0 + \omega)a^{-1} \approx K_0, \quad (28)$$

where $q_n = d^n q/d\omega^n$ at $\omega = \omega_0$. In particular, $q_1^{-1} = v_g$ is the group velocity, while q_2 takes into account the group-velocity dispersion.

Considering expansions (28), we have the following description of the evolution of slowly varying envelopes:

$$i\left(\frac{\partial}{\partial x} + \frac{1}{v_g}\frac{\partial}{\partial t}\right)\mathscr{A} - \frac{q_2}{2}\frac{\partial^2}{\partial t^2}\mathscr{A} + \Delta q_0\mathscr{A} = -K_0\mathscr{P}, \quad (29)$$

$$i\left(\frac{\partial}{\partial x} - \frac{1}{v_g}\frac{\partial}{\partial t}\right)\mathscr{B} + \frac{q_2}{2}\frac{\partial^2}{\partial t^2}\mathscr{B} - \Delta q_0\mathscr{B} = +K_0\mathscr{P}, \quad (30)$$

where $\Delta q_0 = q_0 - 2\pi/a$. The next step requires a choice of a model for the medium of the thin films. Possibilities include anharmonic oscillators, two- or three-level atoms, excitons of molecular chains, nano-particles, quantum dots, and others. First, we consider the two-level atom model.

2.5 Example: Thin Films Containing Two-Level Atoms

Here we employ the approach developed above to derive an already-known system of equations [1]. The model assumes that each thin film contains two-level atoms. The state of a two-level atom is described by a density matrix, $\hat{\rho}$. The matrix element ρ_{12} describes the transition between the ground state, $|2\rangle$, and the excited state, $|1\rangle$.

ρ_{22} and ρ_{11} represent the populations of these states. The evolution of the two-level atom is governed by the Bloch equations [20]:

$$i\hbar \frac{\partial}{\partial t}\rho_{12} = \hbar\Delta\omega\rho_{12} - d_{12}(\rho_{22} - \rho_{11})A_{\text{in}}, \tag{31}$$

$$i\hbar \frac{\partial}{\partial t}(\rho_{22} - \rho_{11}) = 2\left(d_{12}\rho_{21}A_{\text{in}} - d_{21}\rho_{12}A_{\text{in}}^*\right). \tag{32}$$

In these equations, A_{in} is the electric field interacting with a two-level atom. In the problem under consideration, $A_{\text{in}} = \mathscr{A} + \mathscr{B}$, and

$$K_0\mathscr{P} = \frac{2\pi\omega_0 n_{\text{at}}d_{12}}{cn(\omega_0)}\langle\rho_{12}\rangle.$$

Here, the cornerstone brackets denote summation over all atoms within a frequency detuning of $\Delta\omega$ from the center of the inhomogeneity broadening line, $n(\omega_0)$ is the refractive index of the medium containing the array of thin films, and n_{at} is the effective density of the resonant atoms in the films. n_{at} is defined by $n_{\text{at}} = N_{\text{at}}(\ell_{\text{f}}/a)$, where N_{at} is the bulk density of atoms, ℓ_{f} is the film width, and a is the lattice spacing.

We assume that the group-velocity dispersion is of no importance. The resulting equations are the two-wave reduced Maxwell–Bloch equations. We introduce the normalized variables

$$e_1 = t_0 d_{12}\mathscr{A}/\hbar, \quad e_2 = t_0 d_{12}\mathscr{B}/\hbar, \quad x = \zeta v_g t_0, \quad \tau = t/t_0.$$

The normalized two-wave reduced Maxwell–Bloch equations take the following form:

$$i\left(\frac{\partial}{\partial\zeta} + \frac{\partial}{\partial\tau}\right)e_1 + \delta e_1 = -\gamma\langle\rho_{12}\rangle, \tag{33}$$

$$i\left(\frac{\partial}{\partial\zeta} - \frac{\partial}{\partial\tau}\right)e_2 - \delta e_2 = +\gamma\langle\rho_{12}\rangle, \tag{34}$$

$$i\frac{\partial}{\partial\tau}\rho_{12} = \Delta\rho_{12} - ne_{\text{in}}, \tag{35}$$

$$\frac{\partial}{\partial\tau}n = -4\,\text{Im}(\rho_{12}e_{\text{in}}^*), \tag{36}$$

where $\gamma = t_0 v_g/L_a$, $\delta = t_0 v_g\Delta q_0$, $L_a = (cn(\omega_0)\hbar)/(2\pi\omega_0 t_0 n_{\text{at}}|d_{12}|^2)$ is the resonant absorption length, and $\Delta = \Delta\omega t_0$ is the normalized frequency detuning.

We define $n = \rho_{22} - \rho_{11}$, $e_{\text{in}} = e_1 + e_2$ and introduce yet another change of variables:

$$e_{\text{in}} = e_1 + e_2 = f_s\exp(i\delta\tau), \quad e_1 - e_2 = f_a\exp(i\delta\tau), \quad \rho_{12} = r\exp(i\delta\tau).$$

The system of equations (33), (34), (35), and (36) can be rewritten as

$$\frac{\partial f_s}{\partial \zeta} + \frac{\partial f_a}{\partial \tau} = 0, \tag{37}$$

$$\frac{\partial f_a}{\partial \zeta} + \frac{\partial f_s}{\partial \tau} = 2\mathrm{i}\gamma\langle r \rangle, \tag{38}$$

$$\mathrm{i}\frac{\partial}{\partial \tau}r = (\Delta + \delta)r - nf_s, \tag{39}$$

$$\frac{\partial}{\partial \tau}n = -4\,\mathrm{Im}(rf_s^*). \tag{40}$$

From (37), it follows that

$$\frac{\partial f_a}{\partial \zeta} = -\frac{\partial f_s}{\partial \tau},$$

which allows us to rewrite (37), (38), (39), and (40) in the form

$$\frac{\partial^2 f_s}{\partial \zeta^2} - \frac{\partial^2 f_s}{\partial \tau^2} = -2\mathrm{i}\gamma\left\langle \frac{\partial r}{\partial \tau} \right\rangle, \tag{41}$$

$$\mathrm{i}\frac{\partial}{\partial \tau}r = (\Delta + \delta)r - nf_s, \tag{42}$$

$$\frac{\partial}{\partial \tau}n = -4\,\mathrm{Im}(rf_s^*). \tag{43}$$

If we assume that inhomogeneous broadening is absent, i.e., if the hypothesis of a sharp atomic resonant transition is true, then $\delta + \Delta = 0$, and this system reduces to the Sine–Gordon equation [1]. Reference [4] presents the steady-state solution of (41), (42), and (43) with inhomogeneous broadening taken into account.

2.6 Thin Films Containing Metallic Nano-particles

It was shown above that the counter-propagating electric field waves $\mathscr{A}$ and $\mathscr{B}$ in the slowly varying envelope approximation satisfy the following system of equations:

$$\mathrm{i}\left(\frac{\partial}{\partial x} + \frac{1}{v_g}\frac{\partial}{\partial t}\right)\mathscr{A} - \frac{q_2}{2}\frac{\partial^2}{\partial t^2}\mathscr{A} + \Delta q_0 \mathscr{A} = -\frac{2\pi\omega_0}{c\sqrt{\varepsilon}}\langle \mathscr{P} \rangle, \tag{44}$$

$$\mathrm{i}\left(\frac{\partial}{\partial x} - \frac{1}{v_g}\frac{\partial}{\partial t}\right)\mathscr{B} + \frac{q_2}{2}\frac{\partial^2}{\partial t^2}\mathscr{B} - \Delta q_0 \mathscr{B} = +\frac{2\pi\omega_0}{c\sqrt{\varepsilon}}\langle \mathscr{P} \rangle, \tag{45}$$

where $\Delta q_0 = q_0 - 2\pi/a$ is the mismatch between the carrier wave-number and the Bragg resonance wave-number. To describe the evolution of material polarization in

the slowly varying amplitude approximation, we must model the response of the thin films to an external light field. Previous work has considered various mechanisms as sources of the dielectric properties of metamaterials. In the simplest case, dielectric properties can be attributed to plasmonic oscillations, which are modeled by Lorentz oscillators. Magnetic properties can be described by the equations of a system of LC-circuits [21, 22, 23, 24, 25]. The simplest generalizations of this model include anharmonicity of plasmonic oscillations [13, 27] and the addition of a nonlinear capacitor into each LC-circuit [28]. In this chapter, we consider an array of non-magnetic thin films containing metallic nano-particles which have a cubic nonlinear response to external fields [13, 14, 26].

The macroscopic polarization, P, is governed by the equation

$$\frac{\partial^2 P}{\partial t^2} + \omega_{\mathrm{d}}^2 P + \Gamma_{\mathrm{a}} \frac{\partial P}{\partial t} + \kappa P^3 = \frac{\omega_{\mathrm{p}}^2}{4\pi} E,$$

where ω_{p} is plasma frequency and ω_{d} is the dimension quantization frequency for nano-particles. Losses related to the plasmonic oscillations are taken into account by the parameter Γ_{a}. It is assumed that the duration of the electromagnetic pulse is short enough so that dissipation effects can be neglected. If the anharmonic parameter κ is equal to zero, then we have the famous Lorentz model which describes electromagnetic wave propagation and refraction in metamaterials [21, 22, 23, 24, 25, 29, 30].

Starting from the slowly varying envelope approximation, standard manipulation leads to

$$\mathrm{i}\frac{\partial \mathscr{P}}{\partial t} + (\omega_{\mathrm{d}} - \omega_0)\mathscr{P} + \frac{3\kappa}{2\omega_0}|\mathscr{P}|^2 \mathscr{P} = -\frac{\omega_{\mathrm{p}}^2}{8\pi\omega_0}\mathscr{E}_{\mathrm{int}}(x,t). \tag{46}$$

The terms varying rapidly in time, which are proportional to $\exp(\pm 3\mathrm{i}\omega_0 t)$, are neglected. In this equation, $\mathscr{E}_{\mathrm{int}}$ is the electric field interacting with the metallic nano-particles. In the problem under consideration, we have $\mathscr{E}_{\mathrm{int}} = \mathscr{A} + \mathscr{B}$.

The sizes and shapes of nano-particles are not uniform because of the limitations of nano-fabrication. In practice, the deviation from a perfectly spherical shape has a much larger impact on a nano-particle's resonance frequency than does variation in diameter. This causes a broadening of the resonance line. The broadened spectrum is characterized by a probability density function, $g(\Delta\omega)$, of deviations, $\Delta\omega$, from some mean value, ω_{res}. When computing the total polarization, all resonance frequencies must be taken into account.

The contributions of the various resonance frequencies are weighted according to the probability density function, $g(\Delta\omega)$. The weighted average is denoted by $\langle\mathscr{P}\rangle$ in (44) and (45). In what follows, $n(\omega_0)$ denotes the refractive index of the medium containing the array of thin films, and n_{np} is the effective density of the resonant nano-particles in the films. As in the model of films containing two-level atoms, the effective density is equal to $n_{\mathrm{np}} = N_{\mathrm{np}}(\ell_{\mathrm{f}}/a)$, where N_{np} is the bulk density of nano-particles, ℓ_{f} is the width of a film, and a is the lattice spacing.

We study a medium–light interaction in which resonance is the dominant phenomenon. Hence the length of the sample is smaller than the characteristic dispersion length. In this case, the temporal second derivative terms in (44), and (45) can

be omitted. The resulting equations are the two-wave Maxwell–Duffing equations. They can be rewritten in dimensionless form using the following rescaling:

$$e_1 = \mathscr{A}/A_0,$$
$$e_2 = \mathscr{B}/A_0,$$
$$p = (4\pi\omega_0/[\sqrt{\varepsilon}\omega_p A_0])\mathscr{P},$$
$$\zeta = (\omega_p/2c)x,$$
$$\tau = t/t_0.$$

Here $t_0 = 2\sqrt{\varepsilon}/\omega_p$, while A_0 is the characteristic amplitude of the counter-propagating fields. In dimensionless form, the two-wave Maxwell–Duffing equations read:

$$i\left(\frac{\partial}{\partial\zeta} + \frac{\partial}{\partial\tau}\right)e_1 + \delta e_1 = -\langle p\rangle,$$

$$i\left(\frac{\partial}{\partial\zeta} - \frac{\partial}{\partial\tau}\right)e_2 - \delta e_2 = +\langle p\rangle, \tag{47}$$

$$i\frac{\partial p}{\partial\tau} + \Delta p + \mu|p|^2 p = -(e_1 + e_2),$$

where $\mu = (3\kappa\sqrt{\varepsilon}/\omega_0\omega_p)(\sqrt{\varepsilon}\omega_p/4\pi\omega_0)^2 A_0^2$ is a dimensionless coefficient of anharmonicity, $\delta = 2\Delta q_0(c/\omega_p)$ is the dimensionless mismatch coefficient, and $\Delta = 2\sqrt{\varepsilon}(\omega_d - \omega_0)/\omega_p$ is the dimensionless detuning of a nano-particle's resonant frequency from the field's carrier frequency.

In a co-ordinate system which is rotating with angular frequency δ,

$$e_1 = f_1 e^{i\delta\tau}, \qquad e_2 = f_2 e^{i\delta\tau}, p = q e^{i\delta\tau},$$

equation (47) becomes

$$i\left(\frac{\partial}{\partial\zeta} + \frac{\partial}{\partial\tau}\right)f_1 = -\langle q\rangle,$$

$$i\left(\frac{\partial}{\partial\zeta} - \frac{\partial}{\partial\tau}\right)f_2 = +\langle q\rangle,$$

$$i\frac{\partial q}{\partial\tau} + (\Delta - \delta)q + \mu|q|^2 q = -(f_1 + f_2). \tag{48}$$

Further simplification of the system (48) can be achieved by introducing new variables

$$f_s = -(f_1 + f_2), \qquad f_a = f_1 - f_2,$$

which allow decoupling of one equation from the system of three equations. In these new variables, the polarization, q, is coupled with only one field variable. Simple transformations give

$$\frac{\partial^2 f_a}{\partial \zeta^2} - \frac{\partial^2 f_a}{\partial \tau^2} = 2i\frac{\partial}{\partial \zeta}\langle q \rangle, \tag{49}$$

$$\frac{\partial^2 f_s}{\partial \zeta^2} - \frac{\partial^2 f_s}{\partial \tau^2} = 2i\frac{\partial}{\partial \tau}\langle q \rangle, \tag{50}$$

$$i\frac{\partial q}{\partial \tau} + (\Delta - \delta)q + \mu|q|^2 q = f_s. \tag{51}$$

As one can see, we have a coupled system of equations for f_s and q.

3 Solitary Wave Solutions

We consider localized solitary wave solutions of (49) in the limit of a narrow spectral line, $\Delta\omega_g/\Delta\omega_s \ll 1$, where $\Delta\omega_s$ and $\Delta\omega_g$ are spectral widths of the signal and spectral line $g(\Delta\omega)$, respectively. In this case, the spectral line can be represented as a Dirac δ-function, $g(\Delta\omega) = \delta(\Delta\omega)$. Equations (49), and (51) can then be rewritten as follows:

$$\frac{\partial^2 f_s}{\partial \zeta^2} - \frac{\partial^2 f_s}{\partial \tau^2} = 2i\frac{\partial q}{\partial \tau}, \tag{52}$$

$$i\frac{\partial q}{\partial \tau} + (\Delta - \delta)q + \mu|q|^2 q = f_s. \tag{53}$$

Scaling analysis of this system shows that solitary wave solutions can be represented as

$$f_s = f_0 F_\Omega(\eta) = \frac{1}{\sqrt{\mu}}\left(\frac{2v^2}{1 - v^2}\right)^{3/4} F_\Omega(\eta),$$

$$q = q_0 Q_\Omega(\eta) = \frac{1}{\sqrt{\mu}}\left(\frac{2v^2}{1 - v^2}\right)^{1/4} Q_\Omega(\eta), \tag{54}$$

$$\eta = \sqrt{\frac{2}{1 - v^2}}(\zeta - v\tau).$$

Here, v is the velocity of the solitary wave, η is a scale-invariant parameter in a co-ordinate system moving with the solitary wave, and functions F_Ω and Q_Ω satisfy the following system of equations:

$$F'' = -iQ', \tag{55}$$

$$-iQ' + \Omega Q + |Q|^2 Q = F. \tag{56}$$

The only dimensionless parameter which remains in the system is

$$\Omega = (\Delta - \delta)\sqrt{\frac{1-v^2}{2v^2}}, \tag{57}$$

which characterizes the deviation of carrier frequency from the plasmonic frequency, ω_p, and the Bragg resonance frequency, ω_{Br}.

The first equation implies that $F' = -iQ +$ constant. We seek a solitary-wave solution, so we assume that F, Q, and their derivatives decay to zero as $|\eta| \to \infty$. Hence the constant is zero, and

$$iF' = Q \,,$$
$$-iQ' + \Omega Q + |Q|^2 Q = F. \tag{58}$$

The system of ordinary differential equations (58) has an integral of motion:

$$|Q|^2 - |F|^2 = \text{constant}.$$

For solutions which decay as $|\eta| \to \infty$, the constant is equal to zero, so

$$|Q|^2 = |F|^2.$$

This allows the following parametrization of the solutions:

$$F(\eta) = R(\eta)e^{i\phi(\eta)}, \quad Q(\eta) = R(\eta)e^{i\psi(\eta)},$$

where R, ϕ, and ψ are real-valued functions satisfying

$$R' = -R\sin(\phi - \psi),$$
$$\phi' = -\cos(\phi - \psi), \tag{59}$$
$$\psi' + \Omega + R^2 = \cos(\phi - \psi).$$

If we set $\Phi = \phi - \psi$, then we have

$$\Phi' - \Omega - R^2 = -2\cos\Phi,$$
$$R' = -R\sin\Phi. \tag{60}$$

Taking the second equation of (60) into account, the first equation can be rewritten as

$$R\frac{d}{dR}(\cos\Phi) - \Omega - R^2 = -2\cos\Phi.$$

If we set $y = \cos\Phi$, then we have

$$R\frac{dy}{dR} + 2y = R^2 + \Omega. \tag{61}$$

The solutions of (61) have the form

$$y = \frac{1}{4}R^2 + \frac{\Omega}{2} + cR^{-2},$$

where c is arbitrary. Since $y = \cos\Phi$, the right-hand side must remain between -1 and 1. As we expect $R \to 0$ as $|\eta| \to \infty$, c must be zero. We have the conservation law

$$\cos\Phi = \frac{1}{4}R^2 + \frac{\Omega}{2}. \tag{62}$$

The substitution of (62) into the second equation of (60) and subsequent integration give the following expression for R:

$$R^2 = \frac{2(4 - \Omega^2)}{\Omega + 2\cosh\left\{\sqrt{4 - \Omega^2}(\eta - \eta_0) + \frac{1}{2}\ln\left(\frac{16}{4 - \Omega^2}\right)\right\}}.$$

The right-hand side is positive and real-valued for all η if, and only if, $-2 < \Omega < 2$. The term $\sqrt{4 - \Omega^2}$ appears so often in what follows that we define $\beta = \sqrt{4 - \Omega^2}$. R^2 then has the form

$$R^2 = \frac{2\beta^2}{\Omega + 2\cosh\{\beta(\eta - \eta')\}}, \tag{63}$$

where we have combined the arbitrary constant η_0 and the logarithm into a single constant (η') in the argument of the hyperbolic cosine. Using the conservation law (62), we obtain an expression for Φ:

$$\Phi = 2\arctan\left(\frac{2 - \Omega}{\beta}\tanh\left\{\frac{1}{2}\beta(\eta - \eta')\right\}\right). \tag{64}$$

Now we integrate $\phi' = -\cos\Phi$ and find

$$\phi = -\frac{\Omega}{2}(\eta - \eta') - \arctan\left(\frac{2 - \Omega}{\beta}\tanh\left\{\frac{1}{2}\beta(\eta - \eta')\right\}\right).$$

Finally, we determine ψ:

$$\psi = \phi - \Phi$$
$$= -\frac{\Omega}{2}(\eta - \eta') - 3\arctan\left(\frac{2 - \Omega}{\beta}\tanh\left\{\frac{1}{2}\beta(\eta - \eta')\right\}\right).$$

This pulse only exists if the value of the parameter Ω is within the interval $-2 < \Omega < 2$. The maximal value of the amplitude of this solitary solution is

$$A = \sqrt{2(2 - \Omega)}.$$

The phases ϕ and ψ are nonlinear. Their behavior is asymptotically linear as $\eta \to \pm\infty$. If $\Omega = 0$, then the limiting values of the phases satisfy

$$|\phi(\infty) - \phi(-\infty)| = \pi/2,$$

$$|\psi(\infty) - \psi(-\infty)| = 3\pi/2.$$

4 Energy Partition

The total energy of the solitary wave is distributed between co/contra-propagating fields and medium polarization. Here we study the energy partition between all these components. Using (49), (50), and the conditions as $|\eta| \to \infty$, one can show that

$$f_a(\eta) = -\frac{1}{v}f_s(\eta) = -\frac{f_0}{v}F(\eta). \tag{65}$$

We are interested in the energies of the dimensionless fields f_1, f_2, and polarization q.

$$f_1 = \frac{1}{2}(f_a - f_s) = -\frac{f_0}{2}\left(\frac{1}{v}+1\right)F,$$

$$f_2 = -\frac{1}{2}(f_s + f_a) = \frac{f_0}{2}\left(\frac{1}{v}-1\right)F,$$

$$q = q_0 Q.$$

To find the energies of forward- and backward-propagating waves, we need to calculate the energy of the solitary wave:

$$E_R = \int_{-\infty}^{+\infty} |F|^2(\eta)\,\mathrm{d}\eta = \int_{-\infty}^{\infty} |Q|^2(\eta)\,\mathrm{d}\eta$$

$$= \int_{-\infty}^{+\infty} R^2(\eta)\,\mathrm{d}\eta = 8\arctan\sqrt{\frac{2-\Omega}{2+\Omega}}. \tag{66}$$

Finally, we have the energies

$$E_{f_1} = \frac{f_0^2}{4}\left(\frac{1}{v}+1\right)^2 E_R, \tag{67}$$

$$E_{f_2} = \frac{f_0^2}{4}\left(\frac{1}{v}-1\right)^2 E_R, \tag{68}$$

$$E_q = q_0^2 E_R. \tag{69}$$

The ratios of energies in the various fields, as well as the polarization, have the following forms:

$$\frac{E_{f_1}}{E_{f_2}} = \left(\frac{1+v}{1-v}\right)^2, \tag{70}$$

$$\frac{E_{f_1}}{E_q} = \frac{1}{2}\frac{(1+v)}{(1-v)}, \tag{71}$$

$$\frac{E_{f_2}}{E_q} = \frac{1}{2}\frac{(1-v)}{(1+v)}. \tag{72}$$

Therefore, energy partitioning is determined by only one parameter, v, which is a dimensionless combination of the main system parameters.

5 Numerical Simulation

The shape and phase of the incident pulse are controllable in a real experimental situation. To model pulse dynamics in a Bragg grating, it is natural to consider an asymptotic mixed initial-boundary value problem for (48). We specify the initial conditions as

$$q(\zeta,\tau) \to 0, \quad f_1(\zeta,\tau) \to 0, \quad f_2(\zeta,\tau) \to 0, \quad \tau \to -\infty, \tag{73}$$

with no incident field at the right edge of the sample and with an incident field at the left edge defined as follows:

$$f_1(-10,\tau) = w\exp(i\theta),$$

$$w = 3.5\exp\left[-\frac{1}{2}\left(\frac{\tau - 3.0}{1.5}\right)^2\right],$$

$$\theta = \arctan\left(\tanh\left[1.5\left(\tau - 3.0\right)\right]\right). \tag{74}$$

In our case, the spatial simulation domain was chosen to be $[-10, 40]$. Parameters $\Delta - \delta$ and μ were set to be

$$\Delta - \delta = 0, \quad \mu = 1. \tag{75}$$

As one can see, in a topological sense, we gave the initial pulse the same configuration of phase as the solitary wave solution. This point is important because,

otherwise, the phase difference cannot relax to the symmetry of the stationary wave which is revealed in (64). As a result, the solution will be unstable if it does not have the correct "topological charge".

The second field boundary condition was as follows:

$$f_2(40, \tau) = 0. \tag{76}$$

In the first simulation, we injected a pulse which was relatively close to the solitary wave solution. The results are shown in Figs. 2, 3, and 4. The amplitude and phase difference varied slightly, as did the pulse shape, which was Gaussian. During the first stage ($t \leq 7$) of evolution, we observed rapid excess energy damping in the radiation of quasi-linear waves in both directions, and relaxation to a
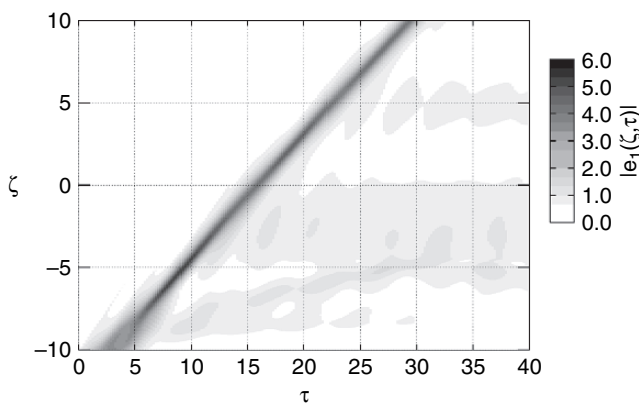
Fig. 2 Propagation of pulse – the first simulation. Mapping of the $|e_1(\zeta, \tau)|$ surface
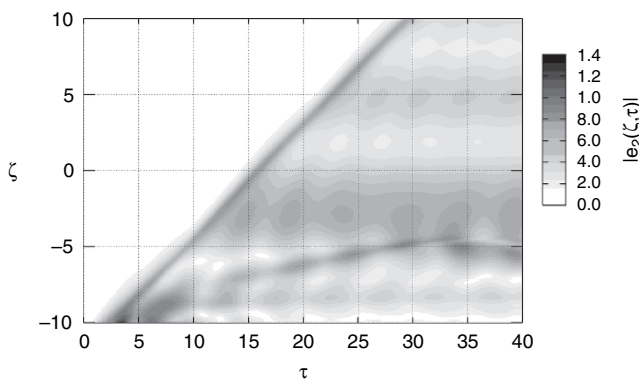
Fig. 3 Propagation of pulse – the first simulation. Mapping of the $|e_2(\zeta, \tau)|$ surface
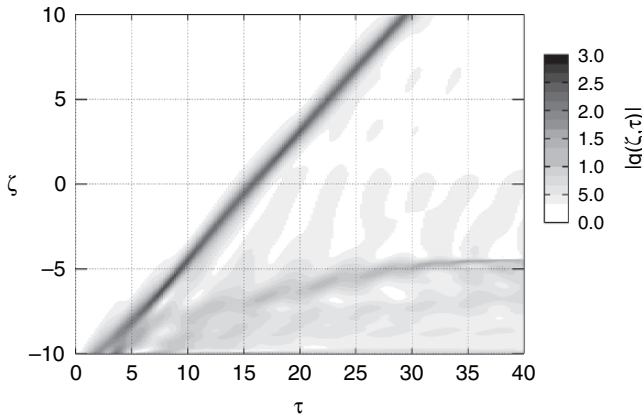
Fig. 4 Propagation of pulse – the first simulation. Mapping of the $|q(\zeta, \tau)|$ surface

solution which roughly approximated a stationary one. Then, we had a stage of pulse shaperefinement ($7 < t < 30$), with consequent propagation of the solution being very close to (63). One can compare the evolved pulse shape with the stationary solution in Fig. 5.

During the second simulation, we used a pulse of lower amplitude:
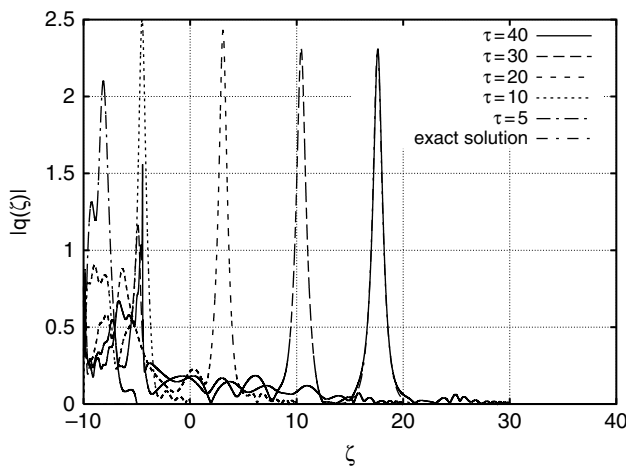
$$f_1(-10, \tau) = w \exp(i\theta),$$

Fig. 5 The first simulation. Absolute value of polarization at different moments of time. The stationary pulse shape almost coincides with the exact solution

$$w = 2.0 \exp\left[-\frac{1}{2}\left(\frac{\tau - 3.0}{1.5}\right)^2\right], \tag{77}$$

$$\theta = \arctan\left(\tanh\left[1.5\left(\tau - 3.0\right)\right]\right). \tag{78}$$

The results are presented in Figs. 6, 7, and 8. The plainly observable oscillations of pulse magnitude can be associated with modes localized in the pulse. This very instructive result could be a fruitful ground for further investigation and simulation.
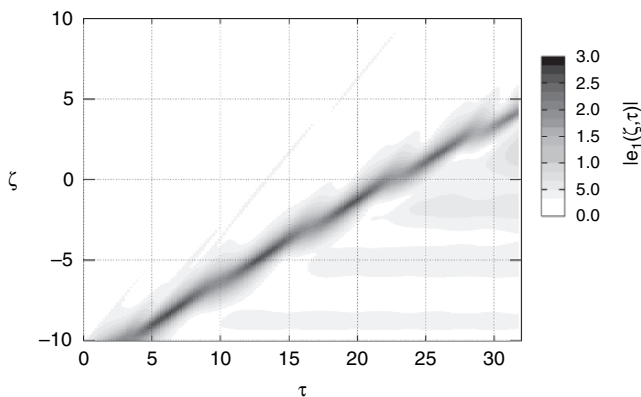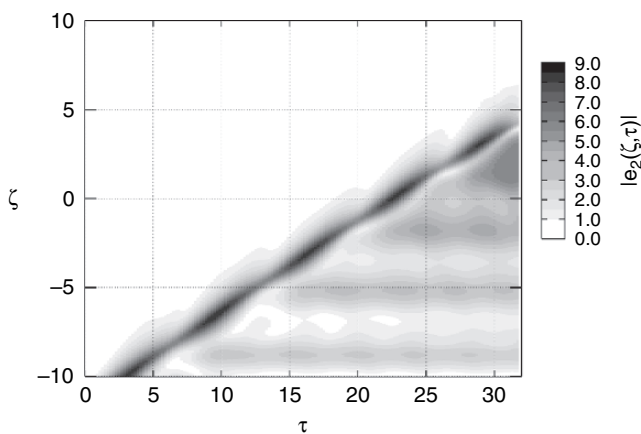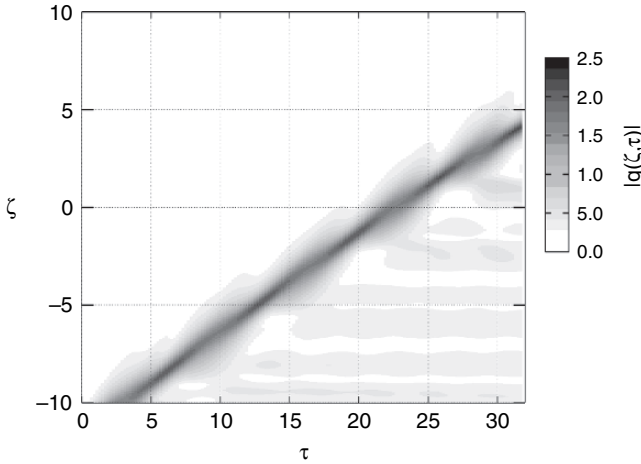

Fig. 6 Propagation of pulse – the second simulation. Mapping of the $|e_1(\zeta, \tau)|$ surface

Fig. 7 Propagation of pulse – the second simulation. Mapping of the $|e_2(\zeta, \tau)|$ surface

Fig. 8 Propagation of pulse – the second simulation. Mapping of the $|q(\zeta, \tau)|$ surface

6 Conclusion

We have derived equations describing optical pulse evolution in Bragg gratings with thin films containing active dopants. In particular, we investigated the case of thin films containing metallic nano-particles. We showed that the system of equations describing this situation has one parameter. This parameter contains information on Bragg and plasmonic frequencies and general pulse characteristics. These equations have solitary wave solutions describing a bound state of two waves propagating in opposite directions with medium polarization.

References

1. B. I. Mantsyzov and R. N. Kuzmin, Sov. Phys. JETP **64**, 37–44 (1986).
2. B. I. Mantsyzov and D. O. Gamzaev, Opt. Spectrosc. **63**, 1, 200–202 (1987).
3. T. I. Lakoba and B.I.Mantsyzov, Bull. Russian Acad. Sci. Phys. **56**, 8, 1205–1208 (1992).
4. B. I. Mantsyzov, Phys. Rev. **A51**, 6, 4939–4943 (1995).
5. B. I. Mantsyzov and E. A. Silnikov, J. Opt. Soc. Amer. B **19**, 2203–2207 (2002).
6. A. Kozhekin and G. Kurizki, Phys. Rev. Lett. **74**, 25, 5020–5023 (1995).

7. A. Kozhekin, G. Kurizki, and B. Malomed, Phys. Rev. Lett. **81**, 17, 3647–3650 (1998).
8. T. Opatrny, B. A. Malomed, and G. Kurizki, Phys. Rev. E **60**, 5, 6137–6149 (1999).
9. G. Kurizki, A. E. Kozhekin, T. Opatrny, and B. A. Malomed, Progr. Opt. **42**, 93–146 (E. Wolf, editor: North Holland, Amsterdam, 2001).
10. J. Cheng and J. Zhou, Phys. Rev. E **66**, 036606 (2002).
11. F. Calogero, A. Degasperis, in *Solitons*, edited by R.K. Bullough, P.J. Caudray, (Springer-Verlag, Berlin, 1980).
12. B. I. Mantsyzov, Optical zoomeron as a result of beatings of the internal modes of a Bragg soliton, JETP Lett. **82**, 5, 253–258 (2005).
13. S.G. Rautian, Nonlinear saturation spectroscopy of the degenerate electron gas in spherical metallic particles, JETP **85**, 451–461 (1997).
14. V.P. Drachev, A.K. Buin, H. Nakotte, and V.M. Shalaev, Size dependent χ^3 for conduction electrons in Ag nanoparticles, Nano Lett. **4**, 1535–1539 (2004).
15. F. Hache, D. Ricard, and C. Flytzanis, Optical nonlinearities of small metal particles: Surface-mediated resonance and quantum size effects, J. Opt. Soc. Am. B **3**, 1647–1655 (1986).
16. V.I. Rupasov and V.I. Yudson, Quantum Electron. (in Russian) **9**, 2179 (1982).
17. V.I. Rupasov and V.I. Yudson, Zh.E.T.Ph. (in Russian) **93**, 494 (1987).
18. P. Yeh, *Optical Waves in Layered Media*, (Wiley, New York, 1988).
19. A.I. Maimistov, A.M. Basharov, *Nonlinear Optical Waves* (Kluwer Academic Publishers, Dordrecht, Boston, London, 1999).
20. L. Allen and J.H. Eberly, *Optical Resonance and Two-Level Atoms*, (Wiley-Interscience, New York, 1975).
21. J.B. Pendry, A.J. Holden, D.J. Robbins, and W.J. Stewart, IEEE Trans. Microw. Theory Tech. **47**, 2075–2084 (1999).
22. D.R. Smith, S. Schultz, P. Markos, and C.M. Soukoulis, Phys. Rev. B **65**, 195104 (2002).
23. N. Katsarakis, T. Koschny, M. Kafesaki, E.N. Economou, and C.M. Soukoulis, Appl. Phys. Lett. **84**, 2943–2945 (2004).
24. P. Markos and C.M. Soukoulis, Phys. Rev. E **65**, 036622 (2002).
25. J.F. Woodley, M.S. Wheeler, and M. Mojahedi, Phys. Rev. E **71**, 066605 (2005).
26. I.R. Gabitov, R.A. Indik, N.M. Litchinitser, A.I. Maimistov, V.M. Shalaev, and J.E. Soneson, J. Opt. Soc. Am. B **23**, 535–542 (2006).
27. N.M. Lichinitser, I.R. Gabitov, A.I. Maimistov, and V.M. Shalaev, Effect of an optical negative index thin film on optical bistability, arXiv. Physics/0607177.
28. A.A. Zharov, I.V. Shadrivov, and Yu.S. Kivshar, Phys. Rev. Lett. **91**, 037401 (2003).
29. R.W. Ziolkowskii and E. Heyman. Phys. Rev. B **64**, 056625 (2001).
30. R.W. Ziolkowski, Optics Express 11 **21167**, 662–681 (2003).